

## One-Electron Singular Branch Lines of the Hubbard Chain

J. M. P. Carmelo<sup>1</sup> ( ), K. Penc<sup>2</sup>, L. M. Martelo<sup>1,3</sup>, P. D. Sacramento<sup>4</sup>, J. M. B. Lopes dos Santos<sup>5</sup>, R. Claessen<sup>6</sup>, M. Sing<sup>6</sup> and U. Schwingenschlogl<sup>6</sup>

<sup>1</sup> GCEP-Center of Physics, U. Minho, Campus Gualtar, P-4710-057 Braga, Portugal

<sup>2</sup> Res. Inst. for Solid State Physics and Optics, H-1525 Budapest, P.O.B. 49, Hungary

<sup>3</sup> Physics Department, Engineering Faculty of U. Porto, P-4200-465 Porto, Portugal

<sup>4</sup> CFI - Instituto Superior Tecnico, Av. Rovisco Pais, 1049-001 Lisboa, Portugal

<sup>5</sup> CFP and Departamento de Física FC U. Porto, P-4169-007 Porto, Portugal

<sup>6</sup> Experimentale Physik II, Universität Augsburg, D-86135 Augsburg, Germany

PACS.71.10.Pm { Fermions in reduced dimensions.

PACS.71.27.+a { Strongly correlated electron systems.

**Abstract.** { The momentum and energy dependence of the weight distribution in the vicinity of the one-electron spectral-function singular branch lines of the 1D Hubbard model is studied for all values of the electronic density and on-site repulsion  $U$ . To achieve this goal we use the recently introduced pseudofermion dynamical theory. Our predictions agree quantitatively for the whole momentum and energy bandwidth with the peak dispersions observed by angle-resolved photoelectron spectroscopy in the quasi-1D organic conductor TTF-TCNQ.

The finite-energy spectral dispersions recently observed in quasi-one-dimensional (1D) metals by angle-resolved photoelectron spectroscopy (ARPES) reveal significant discrepancies from the conventional band-structure description [1,2]. The study of the microscopic mechanisms behind these unusual finite-energy spectral properties remains until now an interesting open problem. There is some evidence that the correlation effects described by the 1D Hubbard model might contain such finite-energy mechanisms [1,2]. However, for finite values of the on-site repulsion  $U$  very little is known about its finite-energy spectral properties, in contrast to simpler models [3]. Bosonization [4] and conformal field theory [5] do not apply at finite energy. For  $U \rightarrow 1$  the method of Ref. [6] provides valuable qualitative information, yet a quantitative description of the finite-energy spectral properties of quasi-1D metals requires the solution of the problem for finite values of  $U$ . The method of Ref. [7] refers to features of the insulator phase. For  $U \rightarrow 4t$ , where  $t$  is the transfer integral, there are numerical results for the one-electron spectral function [8] which, unfortunately, provide very little information about the microscopic mechanisms behind the finite-energy spectral properties. Recent preliminary results obtained by use of the finite-energy holon and spinon description introduced in Refs. [9-11] predict separate one-electron charge and spin spectral branch lines [1]. For the electron-removal spectral function these lines show quantitative agreement with the peak dispersions observed by ARPES in the quasi-1D organic conductor TTF-TCNQ [1]. However,

( ) E-mail: carmelo@fisica.uminho.pt

these preliminary studies provide no information about the momentum and energy dependence of the weight distribution in the vicinity of the charge and spin branch lines and do not describe the TTF dispersion. The main goal of this paper is the evaluation of such a dependence for all values of  $U$  and electronic density. In order to solve this complex many-electron problem, we use the pseudofermion dynamical theory recently introduced in Ref. [12].

The model reads  $\hat{H} = -t \sum_{j,j'} c_{j'}^\dagger c_j + h.c.] + U \sum_j \hat{n}_{j\uparrow} \hat{n}_{j\downarrow}$  where  $c_{j\uparrow}^\dagger$  and  $c_{j\downarrow}$  are spin  $\uparrow, \downarrow$  electron operators at site  $j = 1, \dots, N_a$  and  $\hat{n}_{j\sigma} = c_{j\sigma}^\dagger c_{j\sigma}$ . The low-energy spectral properties of TTF-TCNQ involve inter-chain hopping and electron-phonon interactions. Thus, our results are to be applied above the energies of these processes. We consider an electronic density  $n = N/N_a$  in the range  $0 < n < 1$  and zero magnetization where  $N$  is the electron number. The Fermi momentum is  $k_F = \pi n/2$  and the electronic charge reads  $e$ . The one-electron spectral function  $B^l(k; !)$  such that  $l = -1$  (and  $l = +1$ ) for electron removal (and addition) reads,  $B^{-1}(k; !) = \frac{1}{P} \sum_{\sigma} \langle j | c_{k\sigma}^\dagger j | G S i f^0 (! + E^{N-1}) \rangle$  and  $B^{+1}(k; !) = \frac{1}{P} \sum_{\sigma} \langle j | c_{k\sigma} j | G S i f^0 (! - E^{N_0+1}) \rangle$ . Here  $c_{k\sigma}$  and  $c_{k\sigma}^\dagger$  are electron operators of momentum  $k$  and  $|G S i f^0$  denotes the initial  $N$ -electron ground state. The  $\sum$  and  $\sum_0$  summations run over the  $N-1$  and  $N+1$ -electron excited states, respectively, and  $E^{N-1}$  and  $E^{N_0+1}$  are the corresponding excitation energies.

The pseudofermion dynamical theory reveals and characterizes the dominant microscopic processes which generate over 99% of the electronic weight of the functions  $B^l(k; !)$ , and also describes all other processes [12]. The weight distribution in the vicinity of the branch lines we consider below is fully controlled by such dominant processes. Those involve the  $l=2$  Yang holons and the  $c_0$ ,  $s_1$ , and  $c_1$  pseudofermions studied in Ref. [11]. For simplicity, we denote the first two objects by  $c$  and  $s$  pseudofermions, respectively. The  $c$  pseudofermion carries charge  $e$  and has no spin and the  $s$  pseudofermion is a spin-zero two-spinon composite object and has no charge. The  $c_1$  pseudofermion is a  $l=2$  spin-zero two-holon composite object, carries charge  $2e$ , and has zero spin. The  $l=2$  Yang holon has  $l=2$ ,  $l=2$  spin projection  $l=2$ , charge  $2e$ , and zero spin. The  $c$ ,  $s$ , and  $c_1$  pseudofermions carry momentum  $q = q + Q$  ( $q = N_a$ ), where in our case  $q = c; s; c_1$ . Here  $q$  is the bare momentum and  $Q = q = N_a$  is a momentum functional defined in Ref. [11], whose expression involves the two-pseudofermion phase shifts  $\phi(q; q')$  defined in the same reference, where  $\phi^0 = c; s; c_1$ . Following the one-to-one correspondence between the momentum  $q$  and bare momentum  $q$ , one can either label a pseudofermion by  $q$  or  $q$ . Here we use the bare momentum  $q$ . The above pseudofermions have energy bands  $\epsilon_c(q)$ ,  $\epsilon_s(q)$ , and  $\epsilon_{c_1}(q) = E_u + \epsilon_{c_1}^0(q)$  such that  $|q| \leq k_F$ ,  $|q| \leq k_F$ , and  $|q| \leq 2k_F$ , respectively. These bands are studied and plotted in Ref. [10].  $E_u$  denotes the lower limit of the upper-Hubbard band (UHB) [9] and equals the energy required for creation of a  $l=2$  Yang holon, which is a dispersion-less object. It is such that  $E_u = 4t \cos(\pi n/2)$  for  $U = t \neq 0$ ,  $E_u = U + 4t \cos(\pi n)$  for  $U \gg t$ ,  $E_u = U + 4t$  for  $n \neq 0$ , and as  $n \rightarrow 1$   $E_u$  approaches the value of the Mott-Hubbard gap [10]. In the ground state there are no  $l=2$  Yang holons, the  $c_1$  and  $s$  pseudofermions bands are empty and filled, respectively, and the  $c$  pseudofermions occupy  $0 \leq |q| \leq 2k_F$  (leaving  $2k_F < |q| \leq k_F$  empty).

The ground state and excited states can be expressed in terms of occupancy configurations of the above quantum objects. For electron removal, the dominant processes involve creation of one hole both in  $\epsilon_c(q)$  and  $\epsilon_s(q)$ . For electron addition, these dominant processes lead to two structures: A lower-Hubbard band (LHB) generated by creation of one particle in  $\epsilon_c(q)$  and one hole in  $\epsilon_s(q)$ ; A UHB generated by creation of one hole both in  $\epsilon_c(q)$  and  $\epsilon_s(q)$  and either one particle in  $\epsilon_{c_1}^0(q)$  for  $n < 1$  or one  $l=2$  Yang holon for  $n \rightarrow 1$ . According to the pseudofermion dynamical theory of Ref. [12], both the one-electron spectral-weight singularities and edges are located on pseudofermion branch lines. Such lines are generated by processes where a

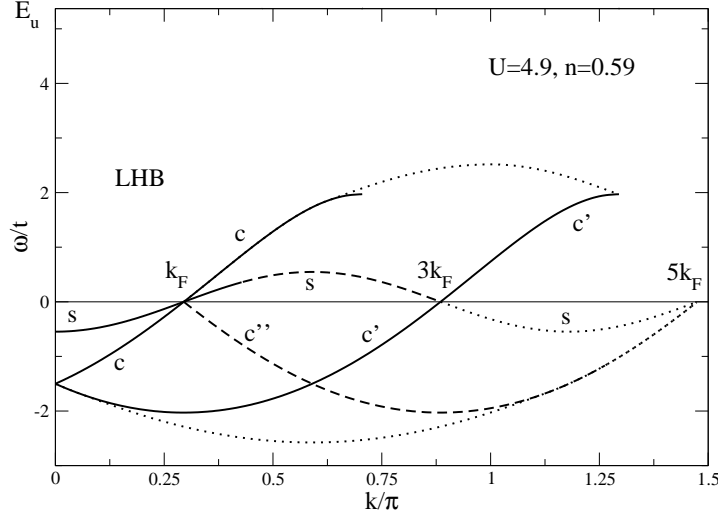


Fig. 1 { Extended-zone scheme centered at  $k = 0$  for  $U = 4.9t$  and  $n = 0.59$ . The solid and dashed lines denoted by the letters  $c$ ,  $c^0$ ,  $c^{00}$ , and  $s$  are singular and edge branch lines, respectively. Electron removal (LHB addition) corresponds to  $! < 0$  (and  $! > 0$ ) and  $! = E_u$  marks the UHB lower limit.

specific pseudofermion is created or annihilated for the available values of bare momentum  $q$  and the remaining quantum objects are created or annihilated at their Fermi points. The weight shape of the singular (and edge) branch lines is controlled by negative (and positive) exponents smaller than zero (and one). The electron removal ( $! < 0$ ) and LHB addition ( $! > 0$ ) singular and edge branch lines are represented in Fig. 1 by solid and dashed lines, respectively. For simplicity, the figure does not represent the  $! > E_u$  UHB region. (Below we find that the shape of the UHB singular branch lines is fully determined by the shape of the electron-removal singular branch lines represented in Fig. 1.) The dashed-dotted lines and some of the branch lines of Fig. 1 are border lines for the  $! < E_u$  domain of the  $(k; !)$ -plane whose spectral weight is generated by dominant processes. (There is a region limited above by the  $s$  line for  $k_F < k < 3k_F$  and below by the  $c^{00}$  and  $c^0$  lines for  $k_F < k < 2k_F$  and  $2k_F < k < 3k_F$ , respectively, which does not belong to that domain.) The dominant processes also include particle-hole pseudofermion processes which lead to spectral weight both inside and outside but in the close vicinity of that domain.

For simplicity, in this letter we consider the exponents that control the weight shape in the vicinity of singular branch lines only. However, similar expressions can be evaluated for any branch line. The singular branch lines correspond to all the  $(k; !)$ -plane regions where there are weight-distribution singularities. While it is difficult to measure the exponents experimentally, a crucial test for the suitability of the model to describe real quasi-1D materials is whether the ARPES peak dispersions correspond to the predicted singular branch lines. The general branch-line spectral-function expression given in Ref. [12] applies provided that the excited states associated with the one-electron branch lines are used.

We start by considering the spin  $s$  branch line for  $0 < k < 3k_F$ , the charge  $c$  branch line for  $0 < k < k_F$ , and the charge  $c^0$  branch line for  $0 < k < k_F + k_F$  (see Fig. 1). The parametric equations that define these branch lines read  $!(k) = s(q)$  for the  $s$  line where  $q = q(k) = (1 + 1)k_F - 1k$  for  $(1 + 1)k_F = 2 < k < k_F + (1 + 1)k_F$  and  $!(k) = c(q)$  for the  $c$  line ( $^0 = +1$ ) and  $! = c^0$  line ( $^0 = -1$ ) where  $q = q(k) = k + ^0k_F$  for  $0 < k < ^0k_F$ .

Here,  $l = -1$  and  $c^0(q) = c(q)$ . The following expression describes the weight distribution in the vicinity of the  $\omega = s; c; c^0$  branch lines for  $l$  values such that  $(-l(q) + 1!)$  is small and positive,

$$B^{-l}(k; ! ) = C^{-l}(k) (-l(q) + 1!)^{(k)} ; \quad \omega = s; c; c^0 : \quad (1)$$

The  $k$ -dependence of  $C^{-l}(k)$ , such that  $C^{-l}(k) > 0$  for  $U=t > 0$ , is in general involved and can be studied numerically. For  $U=t \rightarrow 0$ ,  $C^{-l}(k)$  behaves as  $C_s^{-l}(k) \rightarrow l; -1 C_s$ ,  $C_c^{-l}(k) \rightarrow l; +1 C_c$ , and  $C_{c^0}^{-l}(k) \rightarrow 0$ , where  $C_s$  and  $C_c$  are independent of  $k$ . The exponent of Eq. (1) reads,

$$\begin{aligned} s(k) &= 1 + \sum_{n=1}^{\infty} \ln \frac{1}{2^n} \left[ s_s(k_F; q)^{o_2} + \frac{n}{2^0} + \frac{(1+l)_0}{4} \right] c_s(2k_F; q)^{o_2 i} ; \\ c(k) &= 1 + \sum_{n=1}^{\infty} \ln \frac{f_1(x_0)}{2^n} \left[ s_c(k_F; q)^{o_2} + \frac{n}{4} \right] c_c(2k_F; q)^{o_2 i} ; \end{aligned} \quad (2)$$

where  $\omega = c$  for  $l = +1$ ,  $\omega = c^0$  for  $l = -1$ , and  $f_1(x) = 1 - l(1+x)$ . In equation (2) the phase shifts are defined in Ref. [11] and  $x_0 = \frac{2K}{2K}$  where  $K$  is, such that  $K \rightarrow 1$  as  $U=t \rightarrow 0$  and  $K \rightarrow 1/2$  as  $U=t \rightarrow 1$ , is defined in Ref. [4]. The exponents  $s(k)$  and  $c(k)$  are plotted in Figs. 2 and 3, respectively, as a function of  $k$  for several values of  $U=t$  and  $n = 0.59$ . The exponent  $c(k)$  (and  $c^0(k)$ ) is plotted in Fig. 3 (a) and (b) (and Fig. 3 (c) and (d)) for  $l = -1$  and  $l = +1$ , respectively. As  $U=t \rightarrow 1$  these exponents behave as  $s(k) = 1 + 2(q - 4k_F)^2$  and  $s(k) = (q - 2k_F)[1 - (q - 4k_F)]$  for  $l = -1$  and  $l = +1$ , respectively, and  $c(q) = c^0(q) = 3/8$ , in agreement with Ref. [6]. The weight shape of the UHB singular branch lines is controlled by the same exponents as the corresponding electron-removal branch lines. There is a UHB  $s_u$  branch line for  $k_F < k < \dots$ ,  $c_u$  branch line for  $k_F < k < \dots$ , and  $c_u^0$  branch line for  $3k_F < k < \dots$ . For  $0 < k < \dots$  and  $! > E_u$  the parametric equations of these lines is the same as for the corresponding  $s$ ,  $c$ , and  $c^0$  branch lines, respectively, provided that  $k$  is replaced by  $k$  and  $!$  by  $E_u - !$  in the parametric equations of the latter lines. Under such a replacement the exponents that control the weight shape of these UHB lines are the same as for the corresponding electron-removal lines. While in the limit  $! \rightarrow 1$  such a correspondence refers also to the value of the constant  $C^{-l}(k)$  of Eq. (1), otherwise the corresponding UHB constant  $C_u^{-l}(k)$  is slightly smaller. This is because for  $n < 1$  there is also weight in the vicinity of four UHB  $c_l$  pseudofermion branch lines. We omit here the study of the weight shape of these lines whose exponents are positive.

When the exponents (2) tend to  $-1$  as  $U=t \rightarrow 0$  the expression (1) is replaced by  $(-l(q) + 1!)$ . For  $0 < k < \dots$  and  $U=t \rightarrow 0$  all spectral weight is transferred over to the  $s$  branch line for  $0 < k < k_F$ ,  $c$  branch line for  $k_F < k < k_F$ , and  $s_u$  branch line for  $k_F < k < \dots$ . There is no weight in other branch lines and  $k > 0$  regions of the  $(k; !)$ -plane in such a limit. The two points  $(k = k_F; ! = E_u)$  and  $(k = k_F; ! = c(k))$  where  $q = \dots$  corresponds to  $k = k_F$  become the same point as  $U=t \rightarrow 0$  and the  $c$  and  $s_u$  branch lines become connected at that point. By use of the  $U=t \rightarrow 0$  expressions given in Ref. [10] for  $c(q)$  and  $s(q)$ , one finds that these three branch lines give rise to the electronic spectrum  $! (k) = 2t[\cos(k) - \cos(k_F)]$ . Consistently, the above corresponding exponents are such that  $s(k) \rightarrow -1$  for  $0 < k < k_F$ ,  $c(k) \rightarrow -1$  for  $k_F < k < k_F$ , and  $s_u(k) = s(k) \rightarrow -1$  for  $k_F < k < \dots$  as  $U=t \rightarrow 0$ . Then the correct non-interacting electronic spectral function is reached as  $U=t \rightarrow 0$ . (For  $U=t \rightarrow 0$  the exponents (2) behave as  $s(k) = 1 - 1$ ,  $q = 1 - 1/2 + 1/2$  for  $\omega = c; c^0$  and  $l = -1$ , and  $c(q) = -1$  and  $c^0(q) = 1$  for  $l = +1$ .)

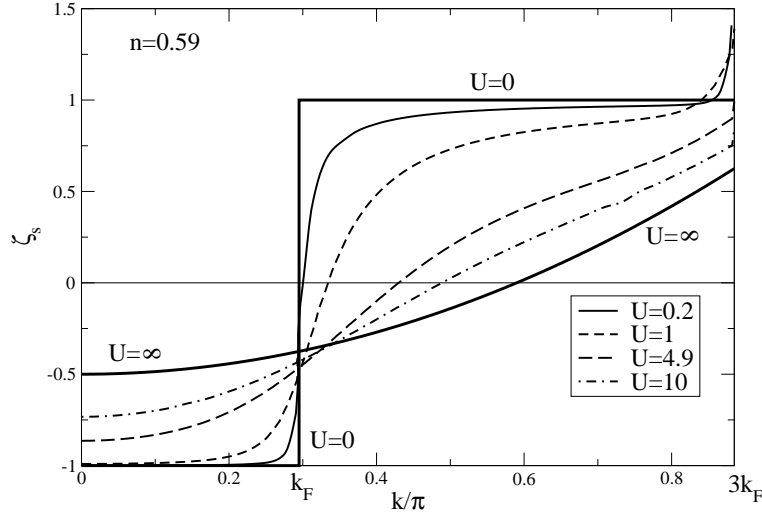


Fig. 2 { Momentum dependence along the spin  $s$  branch line of the exponent (2).

We note that for  $(k; !)$  points in the vicinity of the branch-line end points  $(k_0; jE_u)$  where  $j = 0$  for  $= s_u; c_u^0$  and  $j = 1$  for  $= s_u; c_u; c_u^0$ , respectively, the spectral-function expression (1) remains valid provided that the exponent  $\nu(k)$  given in Eq. (2) is replaced by  $\nu(k) = \nu(k) - 2^{-1}\nu(k)$  for  $! - 1$  ( $q(k) = \nu(k - k_0) + jE_u$ ). Here  $l = 1$ ,  $\nu = \partial(q)/\partial q|_{q=q_F}$ ,  $q_F = 2k_F$ ,  $q_F = k_F$ , and  $2^{-1}\nu(k)$  is a functional defined in Ref. [12]. (In Fig. 1,  $k_0 = k_F$ ,  $k_0 = 3k_F$ , and  $k_0 = 5k_F$  for  $j = 0$ .) For  $j = 0$  this limit corresponds to the so called low-energy Tomonaga-Luttinger liquid regime and the above exponent  $\nu(k)$  equals that given in Eq. (5.7) of Ref. [5]. The branch-line  $k$  domain corresponding to that exponent has zero measure relative to the  $k$  domain of the branch-line exponent  $\nu(k)$ . Therefore, in this paper we do not consider such a limiting regime. Another case of the interest is the behavior of the spectral function in the vicinity of the end points  $(k_0; jE_u)$  when these points are approached by lines which do not cross the branch lines. In this case the weight-distribution is controlled by an exponent different from both  $\nu(k)$  and  $\nu(k)$  [13].

An interesting realization of a 1D metal is the organic charge-transfer salt TTF-TCNQ [2]. The experimental dispersions in the electron removal spectrum of this quasi-1D conductor as measured by ARPES are shown in Fig. 4. The data were taken with He I radiation (21.2 eV) at a sample temperature of 60 K on a clean surface obtained by in situ cleavage of a single crystal. Instrumental energy and momentum resolution amount to 70 meV and  $0.07 \text{ \AA}^{-1}$ , respectively. The experimental data in Fig. 4 reproduce earlier work [1, 2]. While our above theoretical weight-distribution expressions refer to all values of  $U=t$  and  $n$ , we find that the electron removal spectra calculated for  $t = 0.4 \text{ eV}$ ,  $U = 1.96 \text{ eV}$  ( $U/t = 0.49$ ), and  $n = 0.59$  yields an almost perfect agreement with the three TCNQ experimental dispersions. The exception is the low-energy behavior, as a result of the inter-chain hopping and electron-phonon interactions, as mentioned above. If accounted for a renormalization of the transfer integral due to a possible surface relaxation [1], these values are in good agreement with estimates from other experiments [2]. The experimental TCNQ finite-energy peak dispersions of Fig. 4 correspond to the spin  $s$  branch line and charge  $c$  and  $c^0$  branch lines. Importantly, only these singular branch lines, whose weight shape is controlled by negative exponents, lead to peak dispersions in the real experiment. The other peak dispersion of Fig. 4 is associated

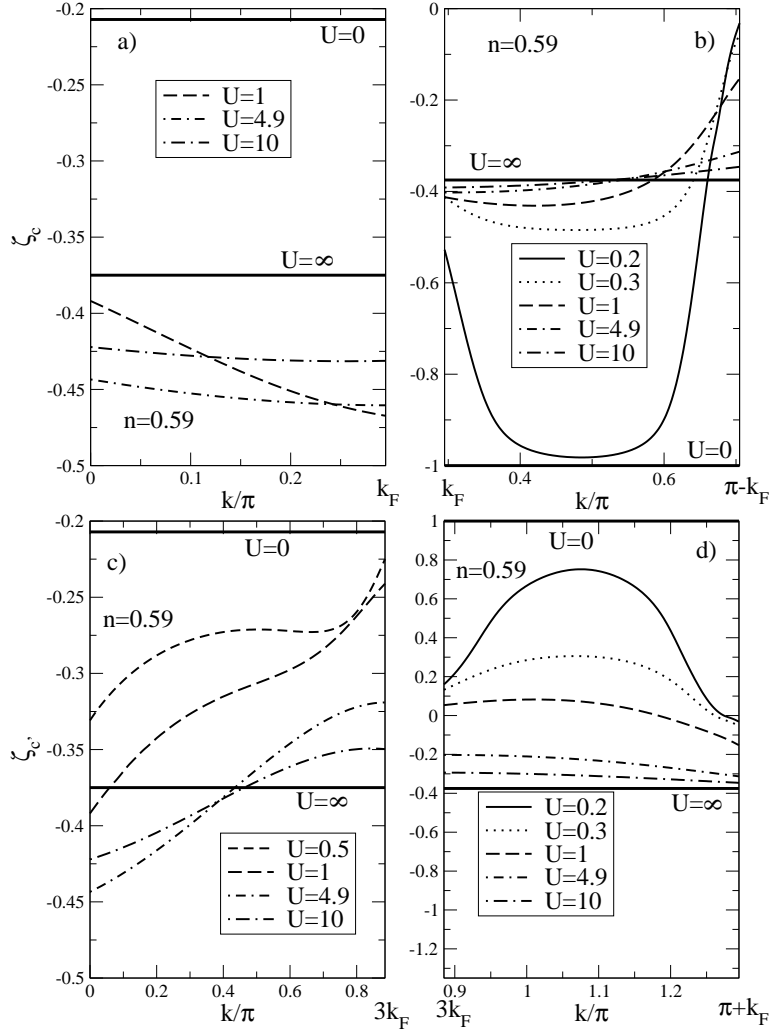


Fig. 3 { Momentum dependence of the exponent (2) along (a) and (c) the electron-removal and (b) and (d) electron-addition charge  $c$  and  $c^0$  branch lines, respectively.

with the electron-removal spectrum of the TTF chains whose density is  $n = 2/0.59 = 1.41$ . It can be described by the electron-addition spectrum of a corresponding  $n = 0.59$  problem. Remarkably, we find again that the theoretical lines match the TTF dispersion provided that  $t = 0.27$  eV and  $U < 0.2t$  within experimental uncertainty. Indeed, for such small values of  $U/t$  and  $n = 0.59$  both the electron-addition exponents of Figs. 2 and 3 (d) are positive, whereas the exponent of Fig. 3 (b) and the UHB exponent  $s_u(k) = s_s(k)$  for  $k < k_F$  (see Fig. 2) are negative. For  $n = 1.41$  the  $c$  and  $s_u$  lines associated with these exponents correspond to electron-removal and thus appear at negative values of  $\epsilon$  and lead to a single singular branch line formed by the  $c$  line for  $0.59/2 < k < 1.41/2$  and the  $s_u$  line for  $1.41/2 < k < \pi$ . The energy pseudogap at  $k = 1.41/2$ , which separates the  $c$  line from the  $s_u$  line, nearly vanishes for  $U/t < 0.2t$  and thus is not observed in the experiment. This singular branch line is that matching the TTF peak dispersion of Fig. 4. (It matches such

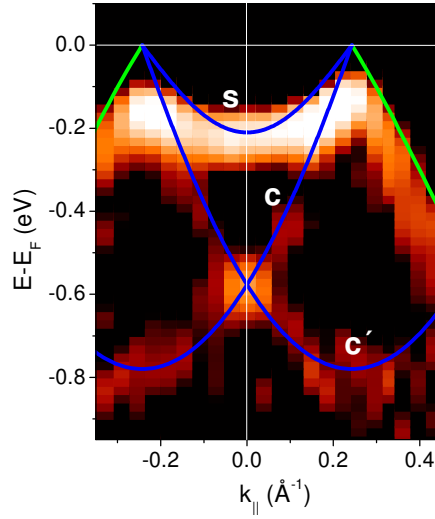


Fig. 4 { Angle-resolved photoemission spectra of TTF-TCNQ measured along the easy transport axis and matching theoretical branch lines.

a dispersion for  $0.59 \approx 2 < k < \dots$ ). We thus conclude that in contrast to the conventional band structure description, the singular branch lines obtained from the 1D Hubbard model describe quantitatively, for the whole finite-energy band width, the peak dispersions observed by ARPES in TTF-TCNQ. This seems to indicate that the dominant non-perturbative many-electron microscopic processes described by the pseudofermion dynamical theory of Ref. [12], which control the weight distribution of these charge and spin singular branch lines, also control the unusual finite-energy one-electron spectral properties of TTF-TCNQ.

We thank E. Jeckelmann for stimulating discussions. K.P. thanks the financial support of OTKA grants D 032689 and T 037451, L.M.M. of FCT grant BD /3797/94, and R.C., M.S., and U.S. of Deutsche Forschungsgemeinschaft (CL 124/3-3 and SFB 484).

#### REFERENCES

- [1] Sing M., Schwingschlogl U., Claessen R., Blaha P., Carmelo J.M.P., Martelo L.M., Sacramento P.D., Dressel M. and Jacobsen C.S., Phys. Rev. B, 68 (2003) 125111.
- [2] Claessen R., Sing M., Schwingschlogl U., Blaha P., Dressel M. and Jacobsen C.S., Phys. Rev. Lett., 88 (2002) 096402; Zwicky F., Jerome D., Margaritondo G., O'Neill

- M., Voit J. and Grioni M., Phys. Rev. Lett., 81 (1998) 2974; Kagoshima S., Nagasawa H. and Sambongi T., One-dimensional conductors (Springer, Berlin) 1987 and references therein.
- [3] Arikawa M., Saiga Y. and Kuramoto Y., Phys. Rev. Lett., 86 (2001) 3096; Penc K. and Shastry B. S., Phys. Rev. B, 65 (2002) 155110.
- [4] Schulz H. J., Phys. Rev. Lett., 64 (1990) 2831.
- [5] Frahm H. and Korepin V. E., Phys. Rev. B, 43 (1991) 5653 and references therein.
- [6] Penc K., Hallberg K., Mila F. and Shiba H., Phys. Rev. Lett., 77 (1996) 1390; *ibid.* Phys. Rev. B, 55 (1997) 15475.
- [7] Sorella S. and Parola A., Phys. Rev. Lett., 76 (1996) 4604.
- [8] Senechal D., Perez D. and Pioro-Ladriere M., Phys. Rev. Lett., 84 (2000) 522.
- [9] Carmelo J. M. P., Roman J. M. and Penc K., Nucl. Phys. B, 683 (2004) 387.
- [10] Carmelo J. M. P. and Sacramento P. D., Phys. Rev. B, 68 (2003) 085104.
- [11] Carmelo J. M. P., cond-mat/0305568.
- [12] Carmelo J. M. P. and Penc K., cond-mat/0311075.
- [13] Carmelo J. M. P., Martelo L. M. and Sacramento P. D., J. Physics: Cond. Matter, 16 (2004) 1375.